Hypertension
JOURNAL OF THE AMERICAN HEART ASSOCIATION
American Heart Association®
Learn and Live℠

Noninvasive Evaluation of Left Ventricular Afterload: Part 1: Pressure and Flow Measurements and Basic Principles of Wave Conduction and Reflection

Julio A. Chirinos and Patrick Segers

Hypertension 2010;56;555-562; originally published online Aug 23, 2010;
DOI: 10.1161/HYPERTENSIONAHA.110.157321
Hypertension is published by the American Heart Association. 7272 Greenville Avenue, Dallas, TX 72514
Copyright © 2010 American Heart Association. All rights reserved. Print ISSN: 0194-911X. Online ISSN: 1524-4563

The online version of this article, along with updated information and services, is located on the World Wide Web at:
http://hyper.ahajournals.org/cgi/content/full/56/4/555

Data Supplement (unedited) at:
http://hyper.ahajournals.org/cgi/content/full/HYPERTENSIONAHA.110.157321/DC1

Subscriptions: Information about subscribing to Hypertension is online at
http://hyper.ahajournals.org/subscriptions/

Permissions: Permissions & Rights Desk, Lippincott Williams & Wilkins, a division of Wolters Kluwer Health, 351 West Camden Street, Baltimore, MD 21202-2436. Phone: 410-528-4050. Fax: 410-528-8550. E-mail:
journalpermissions@lww.com

Reprints: Information about reprints can be found online at
http://www.lww.com/reprints

Downloaded from hyper.ahajournals.org at UNIV ZIEKENHUIS GENT POLIKLIN on October 19, 2010

Noninvasive Evaluation of Left Ventricular Afterload

Part 1: Pressure and Flow Measurements and Basic Principles of Wave Conduction and Reflection

Julio A. Chirinos, Patrick Segers

Abstract—The mechanical load imposed by the systemic circulation to the left ventricle is an important determinant of normal and abnormal cardiovascular function. Left ventricular afterload is determined by complex time-varying phenomena, which affect pressure and flow patterns generated by the pumping ventricle and cannot be expressed as a single numeric measure or described in terms of pressure alone. Left ventricular afterload is best described in terms of pressure-flow relations. High-fidelity arterial applanation tonometry can be used to record time-resolved central pressure noninvasively, whereas contemporary noninvasive imaging techniques, such as Doppler echocardiography and phase-contrast MRI, allow for accurate assessments of aortic flow. Central pressure and flow can be analyzed using simplified biomechanical models to characterize various components of afterload, with great potential for mechanistic understanding of the role of central hemodynamics in cardiovascular disease and the effects of therapeutic interventions. In the first part of this tutorial, we review noninvasive techniques for central pressure and flow measurements and basic concepts of wave conduction and reflection as they relate to the interpretation of central pressure-flow relations. Conceptual descriptions of various models and methods are emphasized over mathematical ones. Our review is aimed at helping researchers and clinicians apply and interpret results obtained from analyses of left ventricular afterload in clinical and epidemiological settings. **(*Hypertension*. 2010;56:555-562.)**

Key Words: afterload ■ noninvasive ■ input impedance ■ arterial load

The mechanical load imposed by the systemic circulation to the pumping ventricle is an important determinant of normal cardiovascular function and plays an important role in the pathophysiology of various cardiac conditions, including hypertensive heart disease, heart failure, postinfarction left ventricular (LV) remodeling, left-sided regurgitant valvular lesions, aortic stenosis, aortic coarctation, and congenital conditions with a systemic right ventricle (eg, congenitally corrected transposition of the great arteries).

LV afterload is the impedance (load) against which the LV must work to promote forward flow (eject blood). In the presence of a normal aortic valve, LV afterload is largely determined by the properties of the arterial tree ("arterial load").[1,2] Although arterial pressure is taken as a useful surrogate of LV afterload in clinical practice, in reality, complex time-varying phenomena determine LV afterload, which ultimately affect, in a reciprocal fashion, the pressure and flow generated by the pumping ventricle. Pressure is not only dependent on afterload but also strongly influenced by ventricular structure and function.[3] Therefore, LV afterload cannot be expressed as a single number, nor can it be described in terms of pressure alone, but should be described in terms of pressure-flow relations, which allow the quantification of "steady" (nonpulsatile) load and various components of pulsatile load.[1,4] Although pulsatile LV afterload is fairly complex, it can be quantified and summarized using relatively simple mechanical models of the systemic circulation. In the first part of this tutorial, we review noninvasive techniques for aortic pressure and flow measurements and describe basic models of pulsatile wave conduction and reflection. In the second part, we review analytic methods used to assess LV afterload using basic physiological principles. Although material properties of the arterial wall (arterial stiffness) are important in cardiovascular disease, we consider them only in the context of their functional consequences for the pumping heart. We refer the reader to excellent literature regarding arterial stiffness,[5,6] which is not the focus of this tutorial. Similarly, it would be impossible to extensively reference landmark contributions from investigators in this area. We cite only general reviews and a limited number of original research publications. Extensive references to original research contributions can be found elsewhere.[1,4]

Noninvasive Pressure Measurements

Arterial applanation tonometry can be used to obtain high-fidelity pressure wave forms from the carotid artery, which is

Received May 31, 2010; first decision June 24, 2010; revision accepted July 29, 2010.

From the Department of Medicine, Philadelphia Veterans' Affairs Medical Center-University of Pennsylvania (J.A.C.), Philadelphia, Pa; Biofluid, Tissue, and Solid Mechanics for Medical Applications (P.S.), IBiTech, Ghent University, Ghent, Belgium.

Correspondence to Julio A. Chirinos, Room 8B-111, University and Woodland Avenues, Philadelphia, PA 19104. E-mail julio.chirinos@uphs.upenn.edu

© 2010 American Heart Association, Inc.

Hypertension **is available at http://hyper.ahajournals.org** **DOI: 10.1161/HYPERTENSIONAHA.110.157321**

Downloaded from hyper.ahajournals.org at UNIV ZIEKENHUIS GENT POLIKLIN on October 19, 2010

morphologically similar to (and, therefore, may be an acceptable noninvasive surrogate of) the aortic pressure wave form.[7] Arterial tonometry is based on the principle that, when the artery is immobilized and the arterial wall is flattened against a pressure sensor, pressure within the lumen is directly transmitted to the sensor. The carotid waveform needs to be calibrated, preferably using mean and diastolic pressure, which can be assessed at the brachial artery.[8] This approach is justified because mean and diastolic pressures exhibit little variation between the upper limb and the central arteries, in contrast to systolic pressure, which increases variably from the aorta to the brachial artery because of the phenomenon of pulse pressure amplification.[1,8] With proper technique, high-fidelity recordings of carotid pressure are feasible in most situations, although great operator skill may be required in some cases, particularly among obese individuals or those with a small stroke volume (ie, heart failure patients). Even with proper technique, high-quality recordings may not be possible in some cases. Technical issues regarding carotid tonometry are discussed in the online Data Supplement, available at http://hyper.ahajournals.org.

For completeness, it is to be mentioned that radial arterial tonometry and application of a transfer function are often used to assess aortic pressure.[1] Although this approach allows for a reliable assessment of central systolic pressure (provided that radial artery waveforms are adequately calibrated), it may be less suited when the central pressure waveform is required in all of its detail, as will be the case here.[9] However, it should also be recognized that there are systematic differences between the carotid and aortic pressure wave forms, such as a greater early systolic carotid upstroke slope compared with the aortic wave form.[10] Although these differences may affect the assessment of specific components of LV afterload (and should be kept in mind), detailed analyses of LV afterload using tonometry-derived carotid pressure closely correlate with those derived from invasive aortic measurements.[11]

Noninvasive Flow Measurements

The 2 most accurate noninvasive techniques for flow measurements in the proximal arterial system are pulsed-wave Doppler (PW-Doppler) echocardiography and cardiac phase-contrast MRI (PC-MRI).[12] Flow measurements with PW-Doppler rely on the principle that the Doppler shift of reflected ultrasound waves induced by moving blood particles is proportional to the velocity of those particles.[1] PW-Doppler is an inexpensive, safe and convenient method to measure flow velocities, and there is widespread expertise in its use (Table). Important technical details for measuring blood flow with PW-Doppler include adequate sample position, sample volume, gain settings, and Doppler beam orientation. Although proximal aortic flow can be difficult to interrogate consistently and reproducibly, LV outflow tract (LVOT) velocities can be adequately interrogated with PW-Doppler in most subjects. Flow velocities must be converted to volume flow by multiplying velocity times LVOT cross-sectional area at the exact point of PW-Doppler interrogation.[1,13,14] This method assumes a flat-flow profile across the LVOT and is highly dependent on the accuracy of cross-sectional area estimations, which in most studies have relied on LVOT anteroposterior diameter measurements from the parasternal long axis view, assuming a circular area (π*radius^2).[13,14] This method has several limitations, including LVOT eccentricity (noncircularity); therefore, our preferred method is 3D echocardiography. Technical tips and considerations for measurements of LVOT velocity and area measurements with PW-Doppler and 3D echocardiography are described in the Data Supplement, figures, and movies available online at http://hyper.ahajournals.org.

Table. Advantages and Disadvantages of Pulsed-Wave Doppler and Phase-Contrast MRI for Measurements of Aortic Flow

Advantages/ Disadvantages	Pulsed Wave Doppler	Phase-Contrast MRI
Advantages	High temporal resolution Low cost Convenience Widespread expertise Easy simultaneous acquisition of pressure waveforms	Measures flow across the entire cross-sectional area Not limited by acoustic windows or anatomic planes Does not assume a flat flow profile
Disadvantages	Limited by acoustic windows Assumes a flat-flow profile Computation of volume flow requires knowledge of vessel cross-sectional area and is therefore subject to considerable error	Lower temporal resolution Cost and inconvenience Less widespread expertise Difficulties in obtaining simultaneous pressure waveforms because of ferromagnetic components in tonometry equipment

PC-MRI relies on the fact that, when 2 opposing magnetic gradient pulses are applied to static nuclei aligned in a magnetic field, the effects of the pulses on nuclear spins cancel each other out, but if a particle moves in the time between the pulses, a phase shift of the nuclear spins within the moving particle is accumulated, which is proportional to the velocity of movement along the gradient's direction. With PC-MRI, velocity maps along any given anatomic plane can be generated. When the gradient direction is applied perpendicular to the cross-sectional vessel plane ("through-plane" velocity encoding; Figure 1), the velocity distribution over the vessel cross-sectional area is measured, without assuming a flat-flow profile. Among other parameters, PC-MRI requires a user-defined velocity-encoding sensitivity, which should be as low as possible to adequately resolve flow velocities, yet higher than peak velocity in the region of interest to avoid aliasing. Although velocity-encoding sensitivity should be tailored to individual measurements, a good starting point for most proximal aortic flow measurements is 130 to 150 cm/s. PC-MRI data are acquired over several cardiac cycles, and consistent cardiac timing in each cycle is assumed. An important technical consideration is that flow measurements may be affected by phase-offset errors caused by in-homogeneities of the magnetic field environment (eddy currents and concomitant gradient effects). Even small background velocity offset errors can result in significant errors in

Downloaded from hyper.ahajournals.org at UNIV ZIEKENHUIS GENT POLIKLIN on October 19, 2010

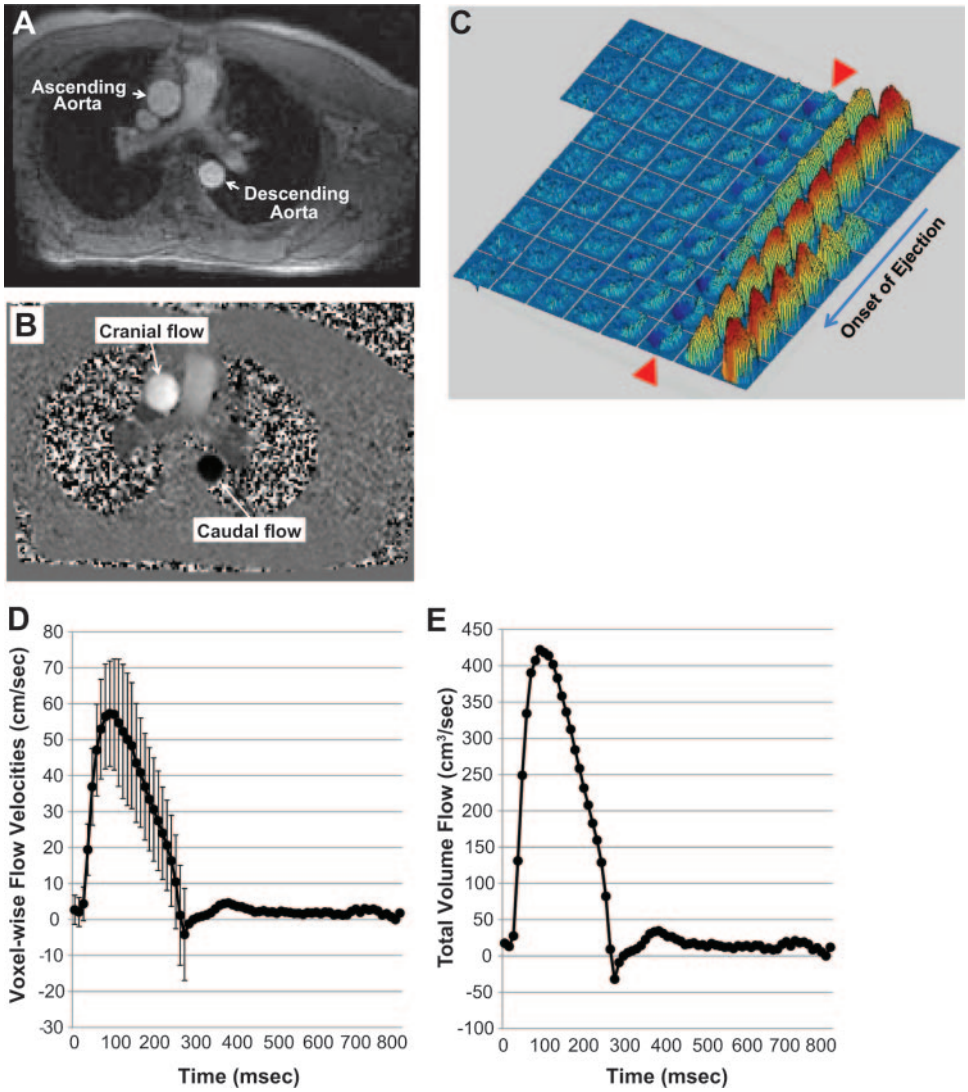

Figure 1. Measurement of proximal aortic flow with PC-MRI. A, Magnitude image. B, Phase image, which represents the through-plane velocity map. C shows the ascending aortic flow profile at various time points. D shows mean flow velocity; bars represent SDs of voxel-wise velocity at each time point during ejection. Note the wide variation in velocity, the nonflat-flow profile, and simultaneous forward (light blue) and backward (dark blue) flow during late systole (arrowheads). E shows net time-resolved volumetric flow. Analyses were performed with the freely available software Segment.[20] See also supplemental movie 5.

volumetric flow, because summation of phase offset across the entire cross-sectional area of the aorta occurs (larger vessels being associated with greater phase-offset errors). The preferred method for phase-offset correction is based on data acquisition from a stationary phantom.[15] If phantom data are not acquired, information from stationary tissue located in the imaging plane[16] may be used to compensate for phase-offset. Other potential problems in PC-MRI that should be kept in mind include signal loss because of turbulent flow and pulsation artifacts. Finally, the anatomic plane should be prescribed exactly perpendicular to the flow direction, parameters should be set to obtain a temporal resolution that meets minimum requirements for planned pressure-flow analytic techniques, and the prescription of the region of interest (aortic lumen) during postprocessing should be as precise as possible. Magnitude images are particularly useful to identify the vessel lumen during systole (because of its high flow-related signal intensity). The precise delineation of the aortic lumen in diastole can be challenging, particularly when magnitude images are used in isolation; matched phase images should always be assessed simultaneously, because they can be very helpful in separating the diastolic lumen (in which low-velocity flow occurs) from the adjacent static tissue. Figure 1 shows an example of through-plane PC-MRI measurements of proximal aortic flow. Table 1 summarizes advantages and disadvantages of PW-Doppler and PC-MRI.

Basic Concepts for Afterload Assessments Using Pressure and Flow Measurements

The terminology "resistance" (R) originates from electric circuit theory and applies to signals that do not vary in time (such as direct current). Ohm's law is well known, with resistance being the ratio of the potential difference (voltage) over a conductor and the electric current. To describe resistance to electric current that fluctuates over time (eg, alternating current), the term impedance (Z) is used. Impedance is a more general formulation than resistance (which it actually includes) but varies with the frequency of fluctuations in the electric signal (R is the value of Z at zero-frequency). These terms have been "borrowed" to describe hemodynamic phenomena.[1,4] Analogous to the dampening of electric flow by electric devices, R and Z in hemodynamics refer to dampening of blood flow by blood vessels, expressing the relation between pressure (voltage) and flow (current). By conven-

Downloaded from hyper.ahajournals.org at UNIV ZIEKENHUIS GENT POLIKLIN on October 19, 2010

tion, the term "resistance" is typically used to describe nonoscillatory opposition to flow, whereas the term "impedance" is used for opposition to fluctuating (pulsatile) flow.

Assuming for the sake of simplicity that the downstream pressure at the end of a vessel of finite length (uniform in geometry and mechanical properties) is 0, resistance to flow imposed by the vessel equals the ratio between mean pressure at its upstream end and mean flow through the vessel (Pm/Qm) and is, according to Poiseuille's law, directly proportional to vessel length and inversely proportional to the fourth power of vessel radius. Impedance to pulsatile flow imparted by a given vessel segment is defined, in analogy, as the ratio of pulsatile change in pressure/pulsatile change in flow in that particular vessel. In the absence of reflected waves in the vessel, this property is called characteristic impedance (Zc). It can be approximated as ρ*PWV/A, where ρ is blood density, pulse wave velocity (PWV) is the propagation speed of the pulse through that vessel, and A is vessel cross-sectional area (which, assuming a circular cross-section, is proportional to radius to the power of 2).[1] PWV (a commonly used index of segmental stiffness), is directly related to the square root of wall elastic modulus and inversely proportional to the square root of vessel radius (ie, radius to the power of 0.5).[4,5,17] Therefore, Zc depends on the stiffness of the vessel but is also highly dependent on vessel radius, being inversely proportional to its power of 2.5.[17]

Input Impedance

The resistance and impedance to flow imposed by a single vessel of finite length or by a vessel segment must be clearly distinguished from the summed resistance/impedance of an entire vascular bed. Because the arterial system is composed of a network of nonuniform, branching vessels with different geometries and wall properties that interact with each other, it is impossible to define the impedance of the arterial system based on single vessel properties. Indeed, the LV only senses the "summed" mechanical load imposed by all of the vessels downstream of the LVOT. The complex pattern of summed impedance imposed by a vascular bed downstream of a particular point (and which can be fully assessed by measuring time-varying flow and pressure at that particular point) is called input impedance[1,4,13,14] (note the difference from characteristic impedance, Zc). Therefore, by analyzing proximal aortic pressure and flow, the impedance of the entire arterial tree is obtained, which is effectively what the heart "sees." Aortic input impedance is, therefore, not a measure of aortic properties but rather reflects the load imparted by the proximal aorta and all of the arterial segments distal to it, including the effects of wave reflections.

Analyses of aortic input impedance are often done in the frequency domain. Any signal with periodicity, as can be reasonably assumed for arterial pressure and flow waves in steady-state (stable) conditions, can be decomposed into its steady (nonpulsatile or zero-frequency) component and its harmonic components, which, by definition, have a frequency that is a multiple of heart rate (fundamental frequency). The mathematical technique used for harmonic decomposition of pressure and flow signals is the Fourier transform.[1,13,14] Each harmonic component is a pure sinusoidal wave with 3 basic

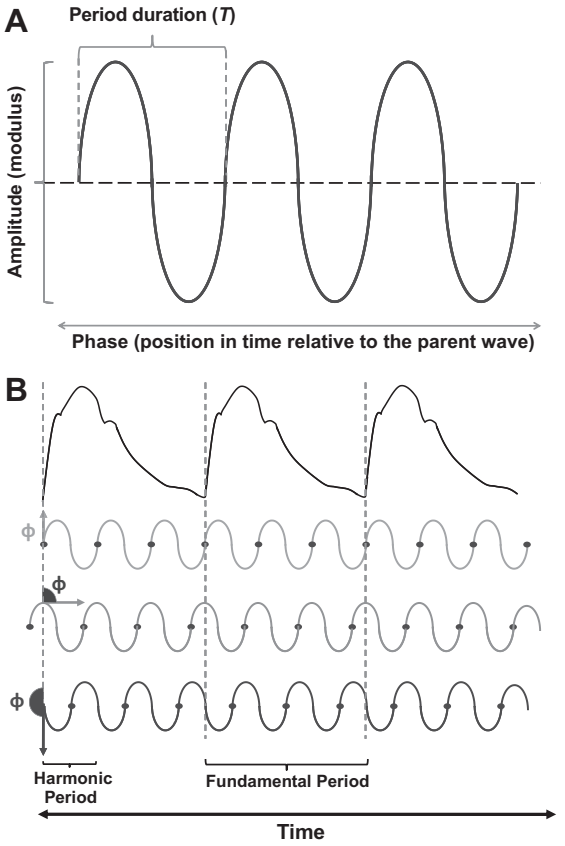

Figure 2. A, Properties of sinusoidal waves: period duration (*T*), amplitude (modulus), and phase angle, which describes the position in time of the sinusoidal wave relative to the parent wave. B shows a pressure waveform and a hypothetical third harmonic of arbitrary amplitude with different phase angles. These hypothetical third harmonics are shown for illustration purposes only and are mutually exclusive and different from the actual pressure wave third harmonic. If the harmonic period starts simultaneously with the fundamental period, phase angle is 0° (top harmonic). If the harmonic is delayed (1/4) of a cycle relative to the parent wave, phase angle is 90° (middle harmonic). If the harmonic is delayed (1/2) a cycle relative to the parent wave, phase angle is 180° (bottom harmonic). A phase angle range of 0° to 360° describes any possible relative position of the harmonic.

properties: modulus (amplitude), period (which determines its temporal frequency, *f*), and phase angle (which is a numeric expression of its position in time relative to the beginning of each fundamental period, or cardiac cycle; Figure 2). When steady and harmonic components of a waveform are added arithmetically, the original waveform is obtained. The number of harmonic components within a waveform that can be discerned depends on the temporal resolution of the acquired signal and equals half the number of time points available within one fundamental period. Most of the energy and relevant details contained in human pressure and flow wave forms are found in the first 10 harmonics, which, therefore, can be obtained if ≥20 measurement points across the cardiac cycle are available.[1] This is an important consideration, because it determines the minimal effective temporal resolution required for flow measurements, which influences prescribed PC-MRI acquisition parameters. As will be discussed in more detail later in this tutorial, once the

Downloaded from hyper.ahajournals.org at UNIV ZIEKENHUIS GENT POLIKLIN on October 19, 2010

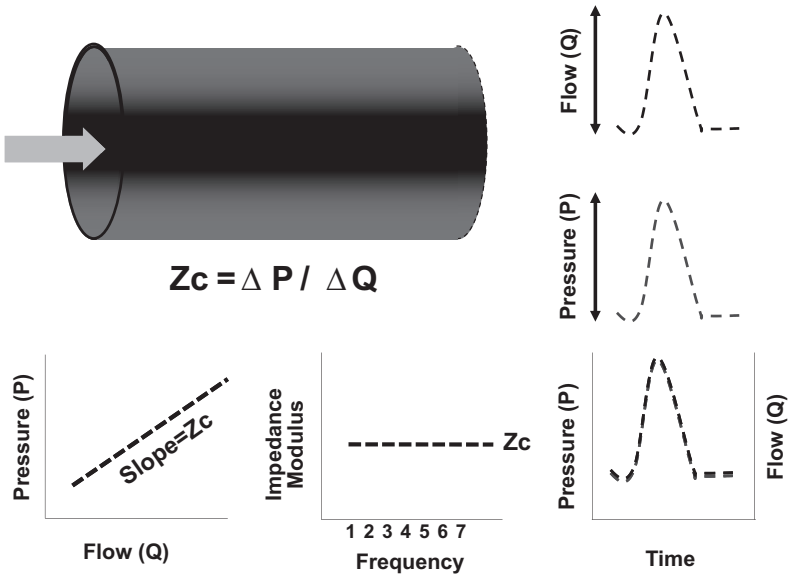

Figure 3. Pulsatile pressure and flow in a single elastic tube of infinite length.

harmonic components of pressure and flow are known, modulus of input impedance is calculated at each frequency as the ratio of pressure modulus/flow modulus, whereas phase angle of input impedance is calculated as pressure phase angle minus flow phase angle ($P\varphi - Q\varphi$).

A more intuitive approach to pressure-flow analyses relies on assessing relationships between pressure and flow waves when these are analyzed "directly" in the time domain rather than decomposed into their harmonics.[1,17] Before further discussing frequency- or time-domain analyses of pressure-flow relations, it is useful to consider extremely simple models of blood flow and pressure in elastic tubes.

Model 1: Pulsatile Pressure and Flow in a Single Elastic Tube of Infinite Length (Absence of Reflected Waves)

The effects of intermittent flow injection into a single elastic tube of infinite length illustrate pressure-flow relations in the absence of reflected waves. Under such conditions, pulsatile energy imparted from one end of the tube promotes forward flow and increases pressure within the tube. Measured flow and pressure signals demonstrate exactly the same shape (Figure 3). The amount of pressure rise (ΔP) versus flow rise (ΔQ; vertical scale in pressure and flow curves in Figure 3) for any given amount of imparted energy is determined by the Zc of the tube (therefore, $Zc = \Delta P/\Delta Q$). The plot of instantaneous pressure versus instantaneous flow data points corresponds to a straight line. The slope of this line is identical to the ratio of $\Delta P/\Delta Q$ and, therefore, represents Zc (Figure 3, bottom left panel); in reality, pressure-flow relations in human vessels are not perfectly linear, but these concepts do apply during early phases of the cardiac cycle. In addition, because pressure and flow wave forms are identical, the amplitude (modulus) of any harmonic relative to the parent wave is identical for pressure and flow, and, therefore, when analyzed in the frequency domain, modulus of input impedance is the same at all of the nonzero frequencies (ie, the ratio between the amplitude of pressure harmonics over the amplitude of the respective flow harmonics is the same for every harmonic pair). This constant impedance modulus is also identical to Zc (Figure 3, bottom middle panel). If Zc is known, pressure and flow can be scaled in the vertical axis and their wave forms superposed (Figure 3, bottom right panel).

Model 2: Pressure and Flow in a Single Elastic Tube of Finite Length in the Presence of Wave Reflections

If we consider an alternative model in which a pulse of flow is injected into an elastic tube of finite length with a "reflector" of the closed-end type at its end (the "impedance" terminating the tube is higher than its characteristic impedance), the energy imparted to the tube promotes forward flow and increases pressure within the lumen. Flow and pressure signals measured during this initial period of time demonstrate exactly the same shape, like in the previous model. Assuming that the fluid within the tube is incompressible (as is the case with blood within vessels), the energy wave imparted to the tube is transmitted along its wall at a finite speed (PWV) until it encounters the reflector on the other side. The energy wave is then reflected and transmitted "backward," promoting flow away from the reflector (backward flow) and an increase in pressure in the lumen. Assuming that no energy loss occurs along the tube and wave reflection is complete (100% of the energy is reflected), the reflected pressure signal is an exact copy of the forward pressure, whereas the flow signal is an exact "negative" version of the original flow (at the site of the reflection, the net pressure doubles, whereas net flow is 0). Therefore, the key difference between the forward and backward waves is that the forward wave manifests as increased pressure and flow, whereas the reflected wave manifests as increased pressure and inverse (or decreased forward) flow, the magnitude of pressure increase and backward flow induced by wave reflections being a function of the initial forward energy and the proportion of energy being reflected.

With progressive decreases in tube length or progressive increases in its PWV, progressively greater superimposition of forward and reflected pressure and flow waves occurs.

Downloaded from hyper.ahajournals.org at UNIV ZIEKENHUIS GENT POLIKLIN on October 19, 2010

Eventually, forward and backward components merge into a single wave from which forward versus backward signals may be difficult to discern based on pressure alone or flow alone. However, because, in the absence of wave reflections, pressure and flow wave forms should be identical (as in model 1), differences in the shape of the pressure versus the flow wave forms (which are induced by wave reflections) can be quantified as long as the 2 wave forms can be related quantitatively to each other (ie, properly "scaled" in the vertical axis). This scaling can be achieved if the parameter that describes the quantitative relationship between pulsatile pressure and flow in the absence of wave reflections is known. This parameter is Zc, which can be measured from early pressure and flow data points in the proximal tube, before the reflected wave returns, using the ratio of early $\Delta P/\Delta Q$ or the slope of the early pressure-flow relation. This is the basis for wave separation analysis,[13,18] which is used to quantify reflected waves in the arterial circulation in the time domain, as discussed in part 2 of this tutorial.

The description above is based on analysis of physics of wave reflection in the time domain, but a similar reasoning can be applied for the frequency domain.[1,14] When considering the wave as a composite of sine waves with different frequencies, manifestations of the reflected wave will depend on the frequency of the sine wave considered. If a given harmonic of the incident wave has a wavelength equal to twice the length of the tube (ie, reflection site located at ½ wavelength), the distance traveled by the wave before returning to the point of origin will correspond exactly to a full wavelength of that particular harmonic. Therefore, round-trip transit time corresponds exactly to the harmonic period (Figure 4A), and the reflected harmonic is delayed a full period relative to its forward counterpart. This causes forward and backward harmonics to be in phase. Two sine waves that are in phase, when added, will produce a sine wave of greater amplitude or modulus (constructive interference, Figure 4A, left). On the other hand, when a sine wave is subtracted from a wave that is in phase and has the same frequency, it will cancel it out (destructive interference, Figure 4A, right). Because reflected energy (for a reflection of the closed end type) increases pressure and decreases ("inverts") flow, the former occurs for the pressure harmonic, whereas the latter occurs for the flow harmonic. Therefore, modulus of input impedance (pressure modulus/flow modulus) at that particular frequency will be high. On the other hand, for a harmonic of wavelength equal to 4 times the distance of the tube (reflection site located at ¼ wavelength), round-trip distance corresponds to half a wavelength, round-trip transit time corresponds to half the harmonic period, and the reflected harmonic is therefore delayed half a period relative to the forward harmonic (ie, is 180° out of phase). The reflected pressure harmonic adds to the incident pressure harmonic and cancels it out, whereas the reflected flow harmonic subtracts from the incident flow harmonic, increasing its amplitude (Figure 4B). Therefore, modulus of input impedance at that frequency is minimized. These principles also apply when partial rather than full reflections occur (Figure 5). It follows that input impedance tends to the minima at one-quarter wavelength frequency (and its odd multiples, eg, 3/4 and 5/4) and to the maxima at (1/2) wavelength (2/4) and all of the other even multiples of quarter wavelength (4/4, 6/4, etc), by an amount proportional to the amount of reflected energy. Therefore, the reflected wave in the frequency domain manifests as oscillations of impedance modulus about a mean non-zero value (which is the Zc of the tube). In addition, as illustrated in Figure 5, for frequencies corresponding with 1/4 wavelength (1/4, 1/2, 3/4, etc) the total pressure and flow harmonics are in phase, so that impedance phase angle ($P\varphi - Q\varphi$) is 0. For intermediate frequencies, phase angle varies between −90 (eg, 3/8) and +90° (eg, 5/8). Finally, according to these principles, one can calculate the distance to the reflection site when the lowest frequency corresponding with a phase angle of 0 and impedance minimum are known, as long as the PWV of the tube is also known.

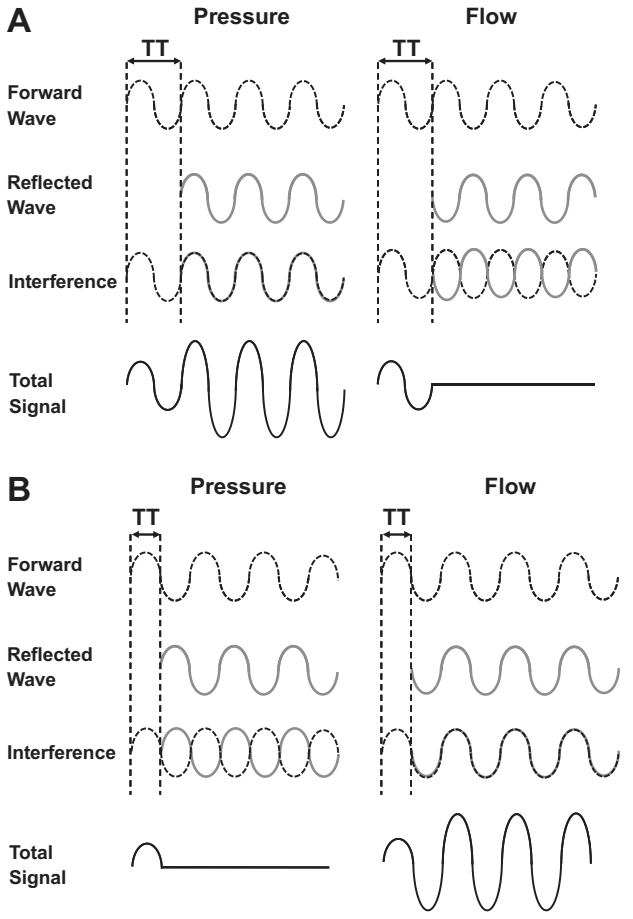

Figure 4. Illustration of constructive and destructive interference as determinants of the "quarter-wavelength rule." When the reflection site is located at (1/2) wavelength, round trip transit time (TT) equals a full period of the harmonic (4A), causing forward and backward harmonics to be in phase, which maximizes the pressure harmonic amplitude, but minimizes the flow harmonic, because the latter it is not only delayed but also "inverted" (negative sign). Impedance modulus (P/Q modulus) at that frequency is maximized. When the reflection site is located at (1/4) wavelength (4B), the round trip TT corresponds with half the harmonic period and the reflected harmonic is 180° out of phase, minimizing the pressure harmonic and maximizing the flow harmonic. Impedance modulus at that frequency is minimized. In this example, reflection of 100% of forward energy is assumed.

Downloaded from hyper.ahajournals.org at UNIV ZIEKENHUIS GENT POLIKLIN on October 19, 2010

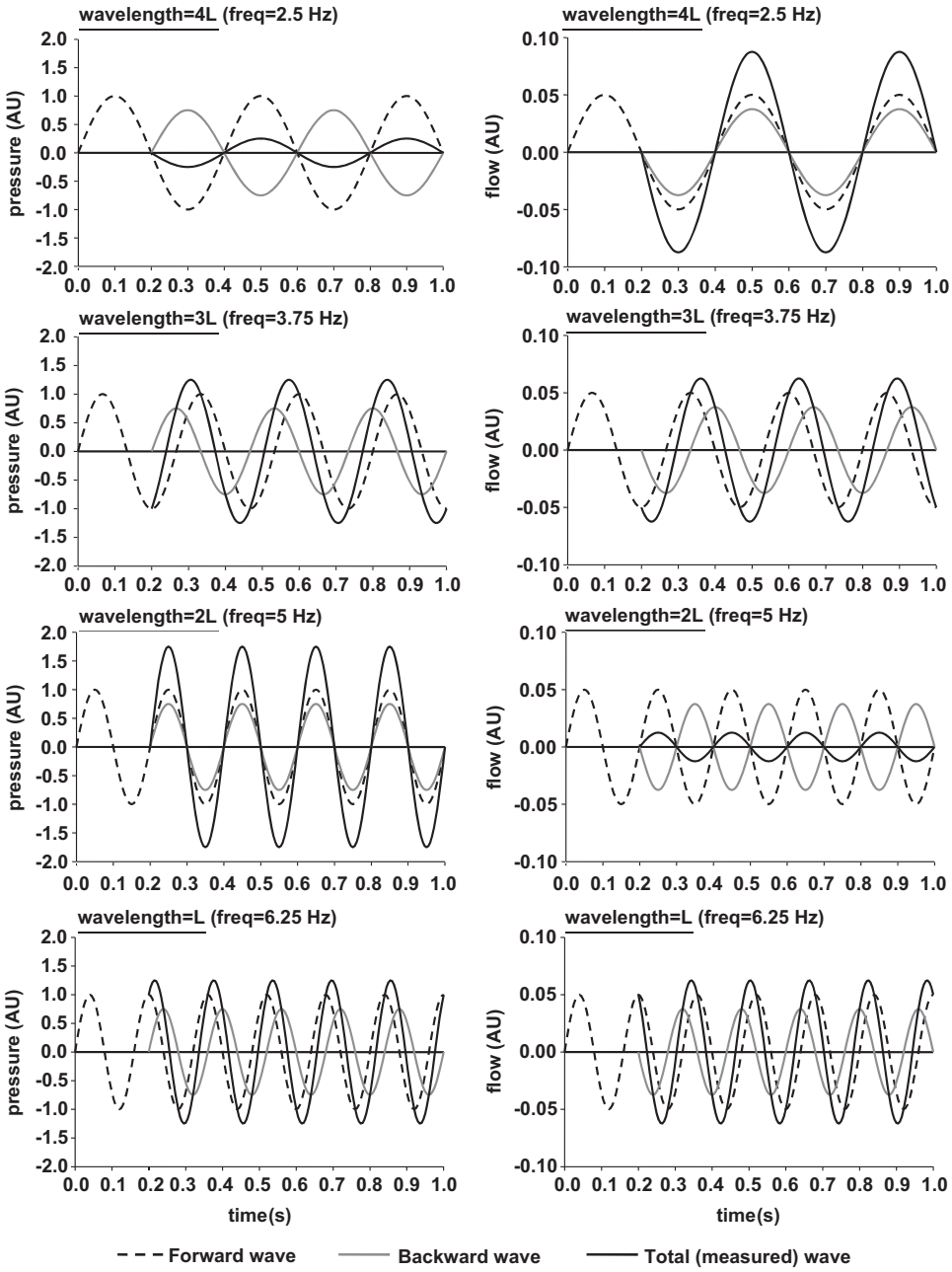

Figure 5. Principle of constructive and destructive interference with partial wave reflection in a tube with length of 1 meter and PWV of 10 m/s. An initial forward wave (dashed line) is generated. In this example, reflection coefficient is 0.75 and the amplitude of the reflected wave (gray line) is 75% of the incident wave amplitude. Total measured pressure harmonics (black continuous lines, left) are the sum of corresponding forward and backward pressure harmonics. Total measured flow harmonics (black continuous lines, right) are the sum of forward and backward flow harmonics. For a frequency of 2.5 Hz (top row), the reflection site is located at (1/4) wavelength (wavelength at PWV of 10 m/s=10/2.5=4 m=4 times the length of the tube). Round trip distance (2 m) equals half a wavelength, round trip transit-time equals half the harmonic period, and the reflected harmonic is delayed half a period relative to the forward harmonic (180° out of phase), with maximal destructive interference for pressure (left), maximal constructive interference for flow (right), and minimal modulus of impedance (not shown). Pressure and flow harmonics have the same phase, and impedance phase (pressure phase minus flow phase) is 0. At a frequency of 5 Hz (third row), wavelength=10/5=2 m. Round-trip distance (2 m) equals a full wavelength, round-trip transit time equals the harmonic period, and reflected and forward harmonics are in phase, with maximal constructive interference for pressure (left), maximal destructive interference for flow (right), and maximal modulus of impedance (not shown). Rows 2 and 4 represent intermediate cases. Pressure amplitude (1.00 AU), flow amplitude (0.05 AU), and Zc (1/0.05=20.00 AU) are expressed in arbitrary units.

Forward and Reflected Waves in the Human Arterial Tree

At the beginning of each cardiac cycle, the heart generates a forward-traveling energy pulse that results in increased pressure and forward flow in the proximal aorta during early systole. If proximal aortic Zc is high because of a stiff wall, a small aortic diameter, or both, the amount of pressure increase is relatively large for any given early systolic flow.[1,14,17] The energy wave generated by the LV (incident wave) is transmitted by conduit vessels and partially reflected

Downloaded from hyper.ahajournals.org at UNIV ZIEKENHUIS GENT POLIKLIN on October 19, 2010

at sites of impedance mismatch, such as points of branching or change in wall diameter or material properties along the arterial tree. Multiple small reflections are conducted back to the heart and merge into a "net" reflected wave, composed of the contributions of the scattered backward reflections. This reflected wave is often looked at as one single discrete wave, originating from an "effective" reflection site (which adheres to the conceptual view of the arterial system as a tube with a single reflection site as described above), but it is important to realize that the reflected wave is the resultant of scattered reflections, originating from distributed reflection sites. The time of arrival of the reflected wave to the proximal aorta depends on the location of reflection sites and on the PWV of conduit vessels, particularly the aorta, which, in turn, is influenced by wall stiffness as described above.[1,14,17] The distance to the reflection sites is strongly dependent on body height. Finally, it should be noted that complex reflection sites may induce phase shifts between the incident and reflected wave that result in differences between the calculated effective reflection distance and the actual anatomic distance to these sites.[19]

Perspectives

Wave conduction and reflections are important determinants of LV afterload and central arterial hemodynamics. Analyses of central pressure-flow relations can be very informative regarding the relatively complex set of events related to wave reflections in the arterial tree, as will be discussed in part 2 of this tutorial.

Disclosures

None.

References

1. Nichols WW, O'Rourke MF. *McDonald's Blood Flow in Arteries. Theoretical, Experimental and Clinical Principles.* 5th ed. London, UK: Oxford University Press; Hodder Arnold; 2005.
2. Kass DA. Ventricular arterial stiffening: integrating the pathophysiology. *Hypertension*. 2005;46:185–193.
3. Segers P, Stergiopulos N, Westerhof N. Quantification of the contribution of cardiac and arterial remodeling to hypertension. *Hypertension*. 2000; 36:760–765.
4. Segers P, Verdonck P. Principles of vascular physiology. In: Lanzer P, Topol E, eds. *Panvascular Medicine: Integrated Clinical Management.* Berlin, Germany: Springer-Verlag; 2002.
5. Laurent S, Cockcroft J, Van Bortel L, Boutouyrie P, Giannattasio C, Hayoz D, Pannier B, Vlachopoulos C, Wilkinson I, Struijker-Boudier H. Expert consensus document on arterial stiffness: methodological issues and clinical applications. *Eur Heart J*. 2006;27:2588–2605.
6. Vlachopoulos C, Aznaouridis K, Stefanadis C. Clinical appraisal of arterial stiffness: the Argonauts in front of the Golden Fleece. *Heart*. 2006;92:1544–1550.
7. Colan SD, Borow KM, Neumann A. Use of the calibrated carotid pulse tracing for calculation of left ventricular pressure and wall stress throughout ejection. *Am Heart J*. 1985;109:1306–1310.
8. Mahieu D, Kips J, Rietzschel ER, De Buyzere ML, Verbeke F, Gillebert TC, De Backer GG, De Bacquer D, Verdonck P, Van Bortel LM, Segers P. Noninvasive assessment of central and peripheral arterial pressure (waveforms): implications of calibration methods. *J Hypertens*. 2010;28: 300–305.
9. Segers P, Rietzschel E, Heireman S, De Buyzere M, Gillebert T, Verdonck P, Van Bortel L. Carotid tonometry versus synthesized aorta pressure waves for the estimation of central systolic blood pressure and augmentation index. *Am J Hypertens*. 2005;18:1168–1173.
10. Chen CH, Ting CT, Nussbacher A, Nevo E, Kass DA, Pak P, Wang SP, Chang MS, Yin FC. Validation of carotid artery tonometry as a means of estimating augmentation index of ascending aortic pressure. *Hypertension*. 1996;27:168–175.
11. Kelly R, Fitchett D. Noninvasive determination of aortic input impedance and external left ventricular power output: a validation and repeatability study of a new technique. *J Am Coll Cardiol*. 1992;20: 952–963.
12. Gatehouse PD, Keegan J, Crowe LA, Masood S, Mohiaddin RH, Kreitner KF, Firmin DN. Applications of phase-contrast flow and velocity imaging in cardiovascular MRI. *Eur Radiol*. 2005;15:2172–2184.
13. Segers P, Rietzschel ER, De Buyzere ML, Vermeersch SJ, De Bacquer D, Van Bortel LM, De Backer G, Gillebert TC, Verdonck PR. Noninvasive (input) impedance, pulse wave velocity, and wave reflection in healthy middle-aged men and women. *Hypertension*. 2007;49:1248–1255.
14. Mitchell GF. Clinical achievements of impedance analysis. *Med Biol Eng Comput*. 2009;47:153–163.
15. Chernobelsky A, Shubayev O, Comeau CR, Wolff SD. Baseline correction of phase contrast images improves quantification of blood flow in the great vessels. *J Cardiovasc Magn Reson*. 2007;9:681–685.
16. Heiberg E, Sjogren J, Ugander M, Carlsson M, Engblom H, Arheden H. Design and validation of Segment: freely available software for cardiovascular image analysis. *BMC Med Imaging*. 10:1.
17. Mitchell GF. Arterial stiffness and wave reflection in hypertension: pathophysiologic and therapeutic implications. *Curr Hypertens Rep*. 2004;6:436–441.
18. Westerhof N, Sipkema P, van den Bos GC, Elzinga G. Forward and backward waves in the arterial system. *Cardiovasc Res*. 1972;6:648–656.
19. Westerhof BE, van den Wijngaard JP, Murgo JP, Westerhof N. Location of a reflection site is elusive: consequences for the calculation of aortic pulse wave velocity. *Hypertension*. 2008;52:478–483.
20. Heiberg E, Markenroth K, Arheden H. Validation of free software for automated delineation and MRI flow analysis. *J Cardiovasc Magn Reson*. 2007;9:375–376.

Downloaded from hyper.ahajournals.org at UNIV ZIEKENHUIS GENT POLIKLIN on October 19, 2010

ONLINE SUPPLEMENT

TITLE: Non-Invasive Evaluation of Left Ventricular Afterload

Part 1: Pressure and Flow Measurements and Basic Principles of Wave Conduction and Reflection

Julio A. Chirinos[1]; Patrick Segers[2].

(1) Philadelphia VA Medical Center and University of Pennsylvania, Philadelphia, PA, USA.

(2) Biofluid, Tissue and Solid Mechanics for Medical Applications (bioMMeda); IBiTech, Ghent University, Belgium.

Address for correspondence
Julio A. Chirinos, MD.
Rm 8B111.
University and Woodland Avenues.
Philadelphia, PA.
email: julio.chirinos@uphs.upenn.edu
Tel +1(215)200-7779.
Fax +1(215)823-5400.

Downloaded from hyper.ahajournals.org at UNIV ZIEKENHUIS GENT POLIKLIN on October 19, 2010

Technical considerations for carotid arterial applanation tonometry

Various technical aspects must be considered to obtain high-fidelity recordings of carotid pressure, which are feasible in most situations. Carotid tonometry is best performed in the supine position. A rolled towel under the neck and slight extension and/or rotation of the subject's head may help bring the carotid artery anteriorly and/or stabilize it between the tonometer and underlying anatomic structures. This maneuver may tighten the skin overlying the artery, particularly among subjects with short necks, impeding adequate flattening of the arterial wall. This can be overcome by relaxation/opening of the jaw. The tonometer can be oriented antero-posteriorly or slightly medially, the latter being useful to take advantage of the support provided by laryngeal cartilage for arterial immobilization. The amount of pressure exerted by the operator on the tonometer should be high enough to acquire a clear signal, but excessive pressure has the potential to result in subject discomfort, vagal responses and/or the inability to record the pressure nadir. The later problem can be detected by the presence of a flat late diastolic pressure profile, rather than the expected asymptotic exponential fall. To minimize error, carotid pressure is typically recorded over several seconds and signal-averaged, because noise decreases as a root function of the number of analyzed beats.

Carotid pressure wave form calibration

The carotid waveform needs to be calibrated, preferably using mean and diastolic pressure (MAP and DBP) which can be assessed at the brachial artery.[1] This approach is justified because MAP and DBP exhibit little variation between the upper limb and the central arteries, in contrast to systolic pressure (SBP), which variably increases from the aorta to the brachial artery due to the phenomenon of pulse pressure amplification[1, 2]. The most accurate method to measure brachial DBP is the auscultatory method, carefully performed by a trained operator, although by itself, this method does not provide MAP. Oscillometric methods accurately measure MAP with less operator dependency but are not as accurate as the auscultatory method to measure DBP.[2] A useful approach is to record a tonometric brachial pressure waveform, which can be calibrated using cuff SBP and DBP determined at the same site.[1] MAP can then be computed via integration of the brachial pressure waveform. However, an adequate brachial pressure waveform recording may not be achievable in all individuals.[3] Several groups have used radial pressure wave forms calibrated with brachial systolic and diastolic pressures to obtain mean arterial pressure via integration of the wave form. This approach may be limited, however, by the considerable and variable degree of brachial to radial amplification[4, 5].

Finally, MAP can be empirically computed from brachial SBP and DBP by adding 40% of pulse pressure to the value of DBP, although this approach carries the risk of systematic error because wave reflections systematically affect the brachial pressure wave form factor (level of MAP relative to SBP and DBP).[1]

Technical considerations for flow measurements with Doppler echocardiography

Important technical details for measuring blood flow with PW-Doppler include adequate sample position, sample volume, gain settings and Doppler beam orientation, which must be perfectly aligned to the direction of blood flow (zero-insonation angle) to avoid underestimation of flow velocities. When a zero-insonation angle is not possible due to anatomic or acoustic window limitations, mathematical corrections can be performed as long as the insonation angle is known, but large offsets from the zero-angle should be avoided. Although proximal aortic flow can be difficult to interrogate consistently and reproducibly, left ventricular outflow tract (LVOT)

Downloaded from hyper.ahajournals.org at UNIV ZIEKENHUIS GENT POLIKLIN on October 19, 2010

velocities can be adequately interrogated with PW-Doppler in most subjects. Flow velocities must be converted to volume flow by multiplying velocity times the cross-sectional area of the LVOT at the exact point of PW-Doppler interrogation.[2, 3, 6] This method assumes a flat flow profile across the vessel lumen and is highly dependent on the accuracy of cross-sectional area estimations. The LVOT tends to be cone-shaped, with the minimal cross-sectional area occurring just below the aortic annulus,[6] although careful examination of LVOT anatomy with 3D-techniques often reveals a slightly more proximal narrowest segment, with widening just underneath the aortic annulus. When PW-Doppler signals are acquired, the point of maximal flow velocities in the LVOT is identified proximal to the aortic valve and the velocity signal from that point is recorded, because according to the continuity equation, this must correspond to the minimal cross-sectional LVOT area, which can be subsequently identified and measured in anatomic images.

Left ventricular outflow tract (LVOT) area measurements

In most studies, LVOT area estimations rely on measurements of the LVOT antero-posterior diameter from the parasternal long axis view (supplemental movie 1), assuming a circular area (π*LVOT radius^2).[3, 6] This method has the following limitations: (1) The anatomic interrogation plane must correspond exactly to the center of the LVOT lumen, or diameter will be underestimated; (2) Errors in diameter measurements are squared during LVOT-area computations; (3) The assumption of a circular LVOT does not hold in most individuals.[7] LVOT shape is almost always elliptical, with the antero-posterior diameter usually being shorter than its orthogonal counterpart (Supplemental Figure-S1). Our preferred approach is the use of full-volume 3D-echocardiography, which can be used for offline multi-planar reconstruction to identify 2 LVOT orthogonal long-axis planes, from which a 3rd plane orthogonal to the first two (true cross-section) can be prescribed (Supplemental Figures S2-3; Supplemental movies 2-4). Freezing the volume in mid-systole and translating the cross-sectional plane allows for the identification of the minimal LVOT cross-sectional area, which can be traced digitally (Supplemental Figure S2B-C). In a recent study among 58 adults, we found a mean 2.98 mm-difference of between the antero-posterior and its orthogonal diameter and a mean 0.4 cm^2-difference between 3D- and 2D-derived LVOT area, although it varied widely, in some subjects being>1 cm^2. Furthermore, there was only a moderate correlation between 2D- and 3D-measurements (R^2=0.58; unpublished data).

Downloaded from hyper.ahajournals.org at UNIV ZIEKENHUIS GENT POLIKLIN on October 19, 2010

References

1. Mahieu D, Kips J, Rietzschel ER, De Buyzere ML, Verbeke F, Gillebert TC, De Backer GG, De Bacquer D, Verdonck P, Van Bortel LM, Segers P. Noninvasive assessment of central and peripheral arterial pressure (waveforms): implications of calibration methods. *J Hypertens.* 2010;28:300-305.
2. Nichols WW and O'Rourke MF. *McDonald's blood flow in arteries. Theoretical, Experimental and Clinical Principles.* . 5 ed: Oxford University Press; 2005.
3. Segers P, Rietzschel ER, De Buyzere ML, Vermeersch SJ, De Bacquer D, Van Bortel LM, De Backer G, Gillebert TC, Verdonck PR. Noninvasive (input) impedance, pulse wave velocity, and wave reflection in healthy middle-aged men and women. *Hypertension.* 2007;49:1248-1255.
4. Verbeke F, Segers P, Heireman S, Vanholder R, Verdonck P, Van Bortel LM. Noninvasive assessment of local pulse pressure: importance of brachial-to-radial pressure amplification. *Hypertension.* 2005;46:244-248.
5. Segers P, Mahieu D, Kips J, Rietzschel E, De Buyzere M, De Bacquer D, Bekaert S, De Backer G, Gillebert T, Verdonck P, Van Bortel L. Amplification of the pressure pulse in the upper limb in healthy, middle-aged men and women. *Hypertension.* 2009;54:414-420.
6. Mitchell GF. Clinical achievements of impedance analysis. *Med Biol Eng Comput.* 2009;47:153-163.
7. Doddamani S, Bello R, Friedman MA, Banerjee A, Bowers JH, Jr., Kim B, Vennalaganti PR, Ostfeld RJ, Gordon GM, Malhotra D, Spevack DM. Demonstration of left ventricular outflow tract eccentricity by real time 3D echocardiography: implications for the determination of aortic valve area. *Echocardiography.* 2007;24:860-866.

Downloaded from hyper.ahajournals.org at UNIV ZIEKENHUIS GENT POLIKLIN on October 19, 2010

Supplemental Figure S1. In this cardiac computed tomography (CT) scan, the antero-posterior LVOT diameter (yellow line) is shown as measured from the LVOT view (which is equivalent to the echocardiographic parasternal long axis view; supplemental Movie 1). This anatomic plane, as shown on the top left panel of Figure S1, corresponds closely to the green diameter on the bottom-right image (2.25 cm), which shows a properly prescribed cross-section of the LVOT. Notice that the LVOT is highly eccentric (not circular) and that the antero-posterior LVOT diameter (green line) is much shorter than its orthogonal diameter (2.9 cm; purple line), which cannot evaluated from the 2D-LVOT view (or parasternal long axis view). In this particular case, assumption of circularity would lead to an estimated LVOT area of 3.8 cm, whereas true cross-sectional area is 4.97 cm^2.

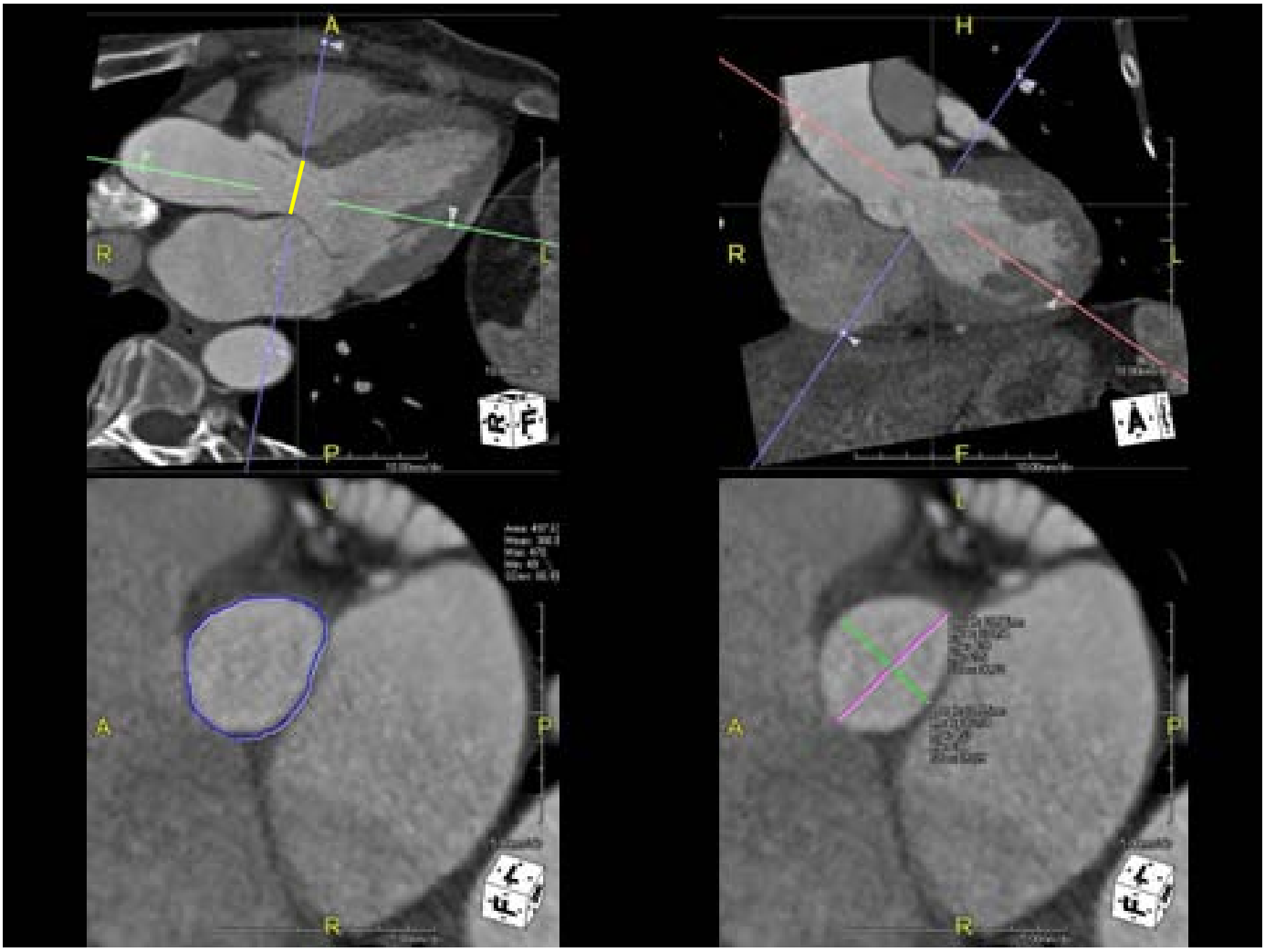

Downloaded from hyper.ahajournals.org at UNIV ZIEKENHUIS GENT POLIKLIN on October 19, 2010

Supplemental Figure S2. Figure S2A shows a full volume of the LVOT obtained with 3D-echocardiography from the parasternal window (also see Supplemental Movie 2). The volume was used for off-line multiplanar reconstruction, which allows for the prescription of 2 LVOT orthogonal long axis planes and a true LVOT cross-sectional plane. The volume allows visualization of multiple parallel slices. Figure S2B and Supplemental Movie 3 shows these parallel planes from a plane distal to the aortic valve/annulus (top panels) to several LVOT cross-sectional planes (below the aortic annulus). These can be used to identify the narrowest LVOT cross-sectional area during ejection (Figure S2C, Supplemental Movie 4), which can then be traced digitally, as shown.

Supplemental Figure S2A (also see Supplemental Movie 2).

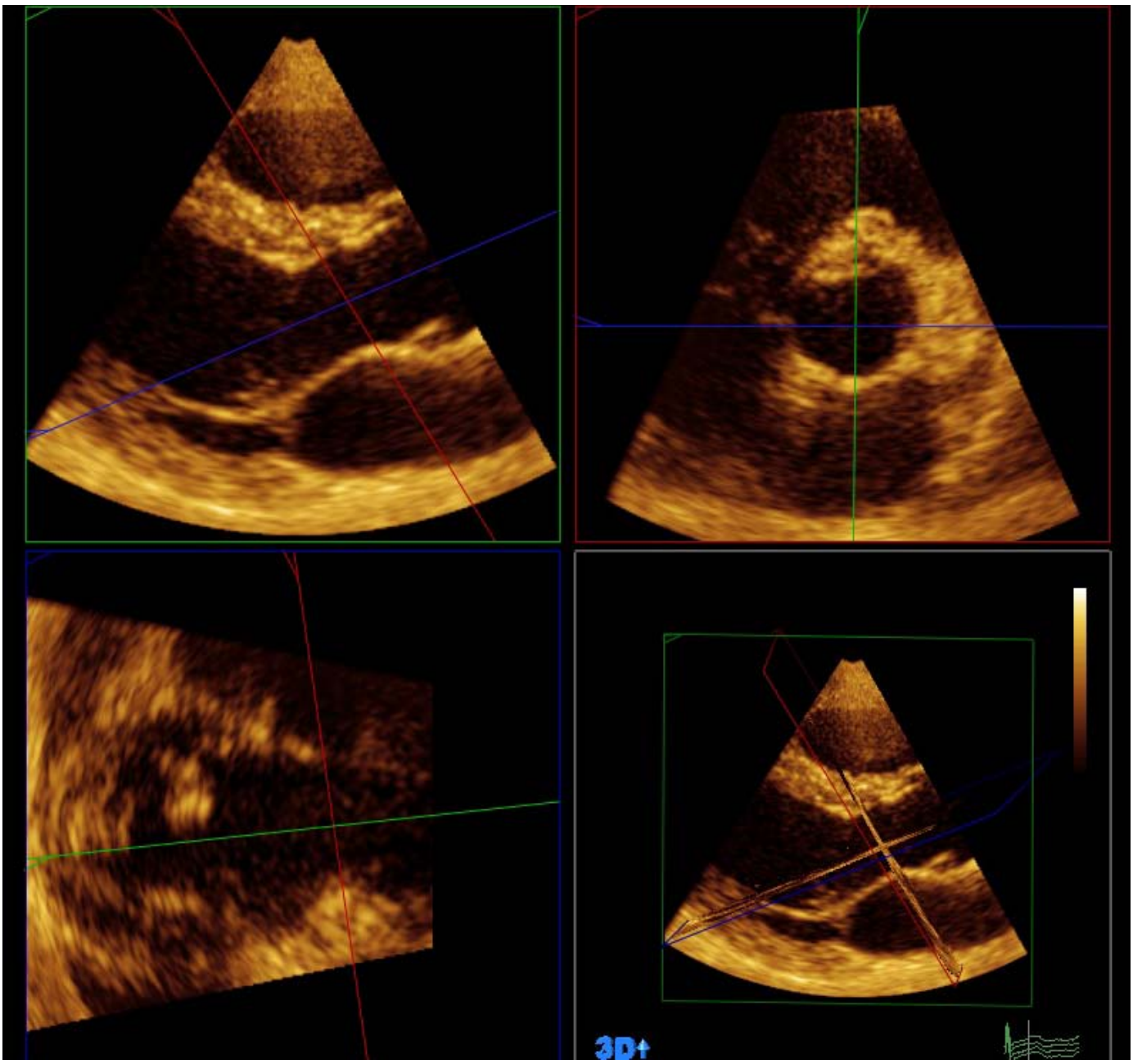

Downloaded from hyper.ahajournals.org at UNIV ZIEKENHUIS GENT POLIKLIN on October 19, 2010

Supplemental Figure S2B. (See also Supplemental Movie 3).

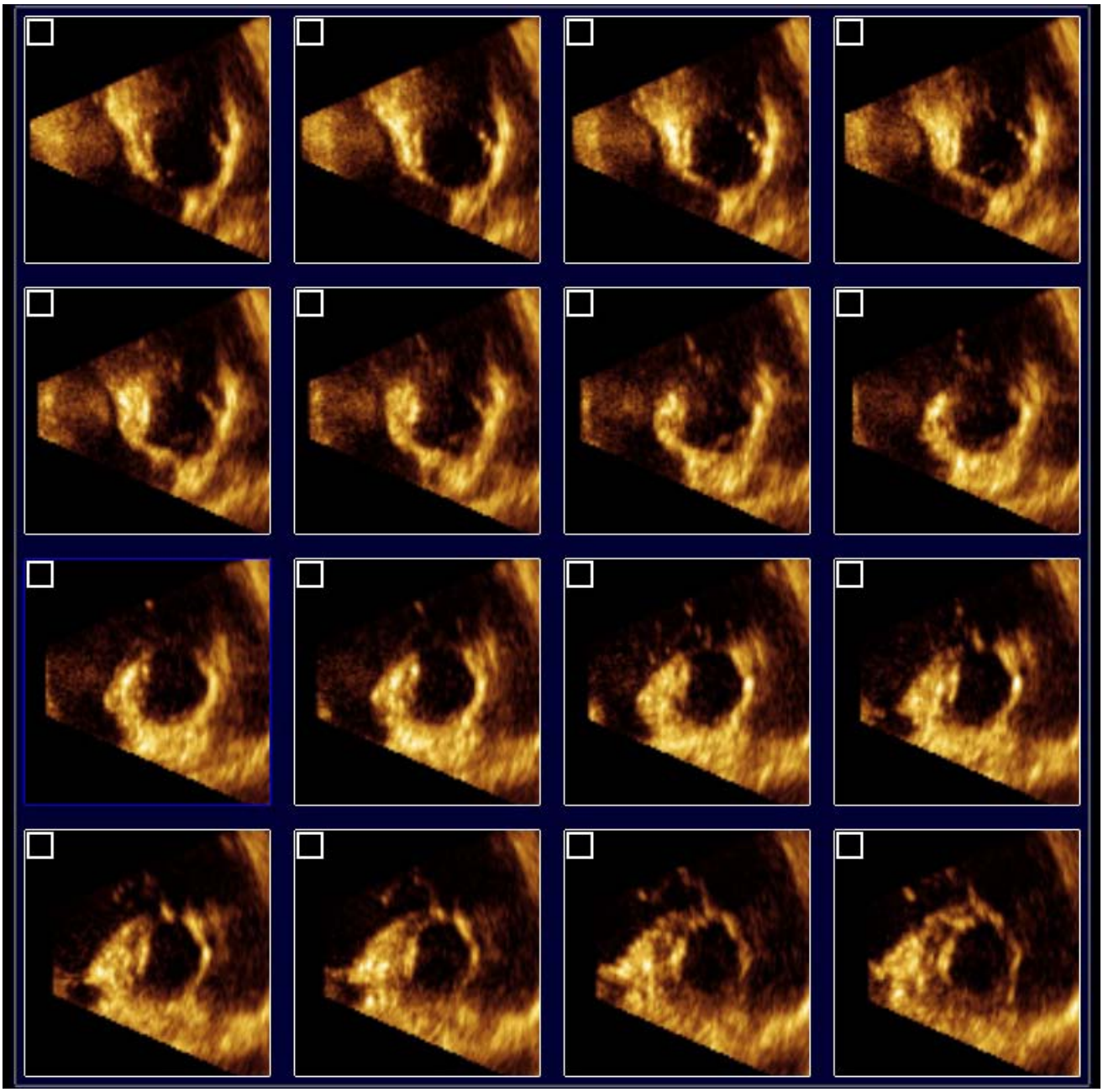

Downloaded from hyper.ahajournals.org at UNIV ZIEKENHUIS GENT POLIKLIN on October 19, 2010

Supplemental Figure S2C. (See also Supplemental Movie 4).

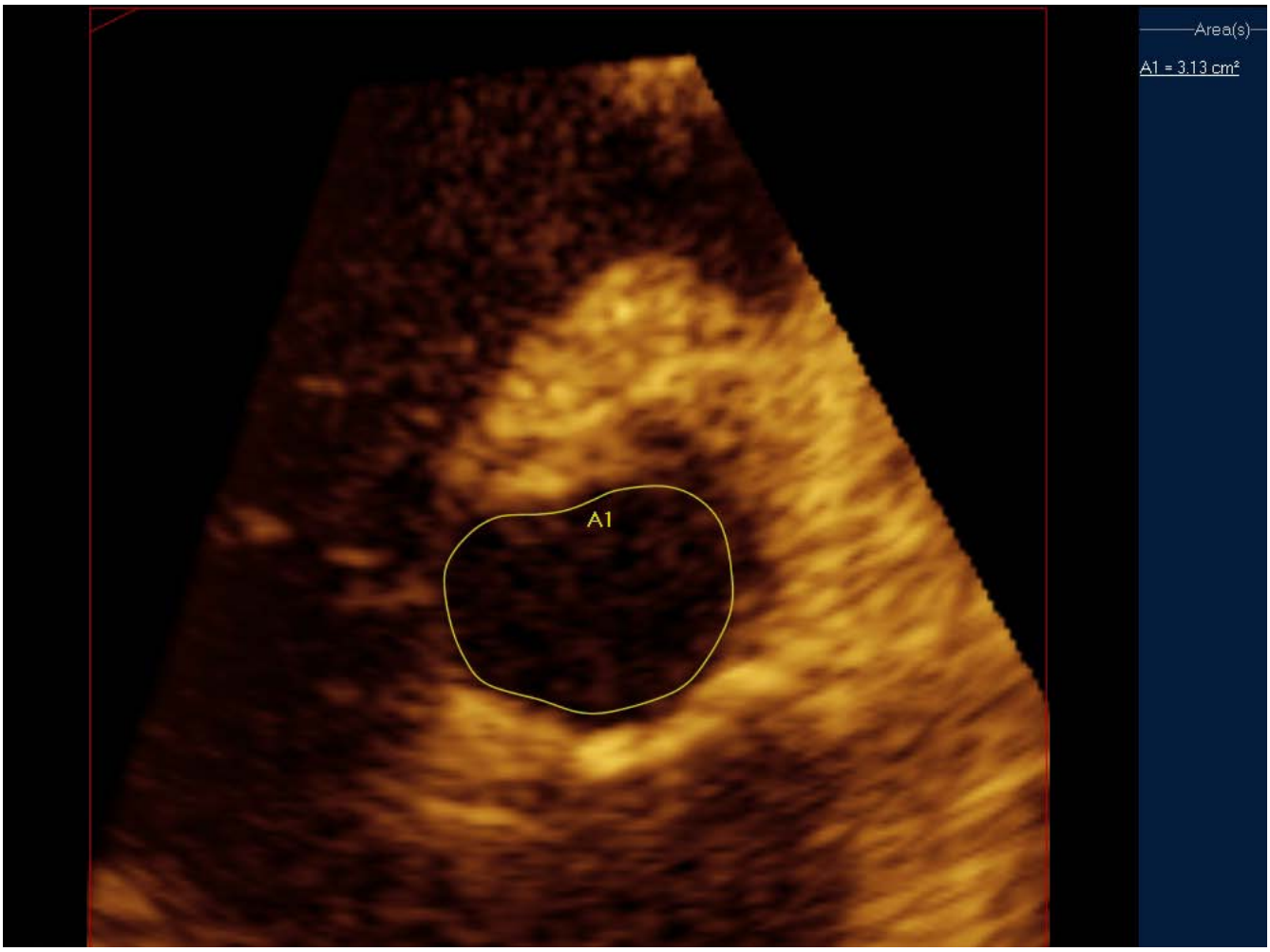

Downloaded from hyper.ahajournals.org at UNIV ZIEKENHUIS GENT POLIKLIN on October 19, 2010

Supplemental Figure S3. Although a parasternal full volume is optimal to assess LVOT anatomy, an apical full volume may occasionally be useful to measure LVOT area in cases in which the parasternal window is not adequate. The figure represents a stepwise multiplanar reconstruction approach than can be followed to prescribe an adequate anatomic LVOT cross-sectional plane, starting from a long axis view of the heart. For clarity, CT images are used. In initial steps, 2 orthogonal long-axis planes (4 chamber and 2-chamber views) should be prescribed that are parallel to the long axis of the left ventricle and pass through the ventricular apex (Steps 1-3). A plane orthogonal to these 2 long-axes planes (a short axis left ventricular plane) is then prescribed and translated to the ventricular base, where the LVOT can be identified (Step 4). A plane is then prescribed across the middle of the LVOT. This yields an "LVOT view", equivalent to the parasternal long axis view. The LVOT long axis can then be identified and prescribed in this view (Step 5), yielding an orthogonal LVOT view in which a second long axis can be identified (Step 6). Once the 2 orthogonal LVOT long axes are known, a third plane orthogonal to these 2 will yield the cross-section of the LVOT. This plane can be translated to identify the narrowest LVOT area during ejection (Step 7).

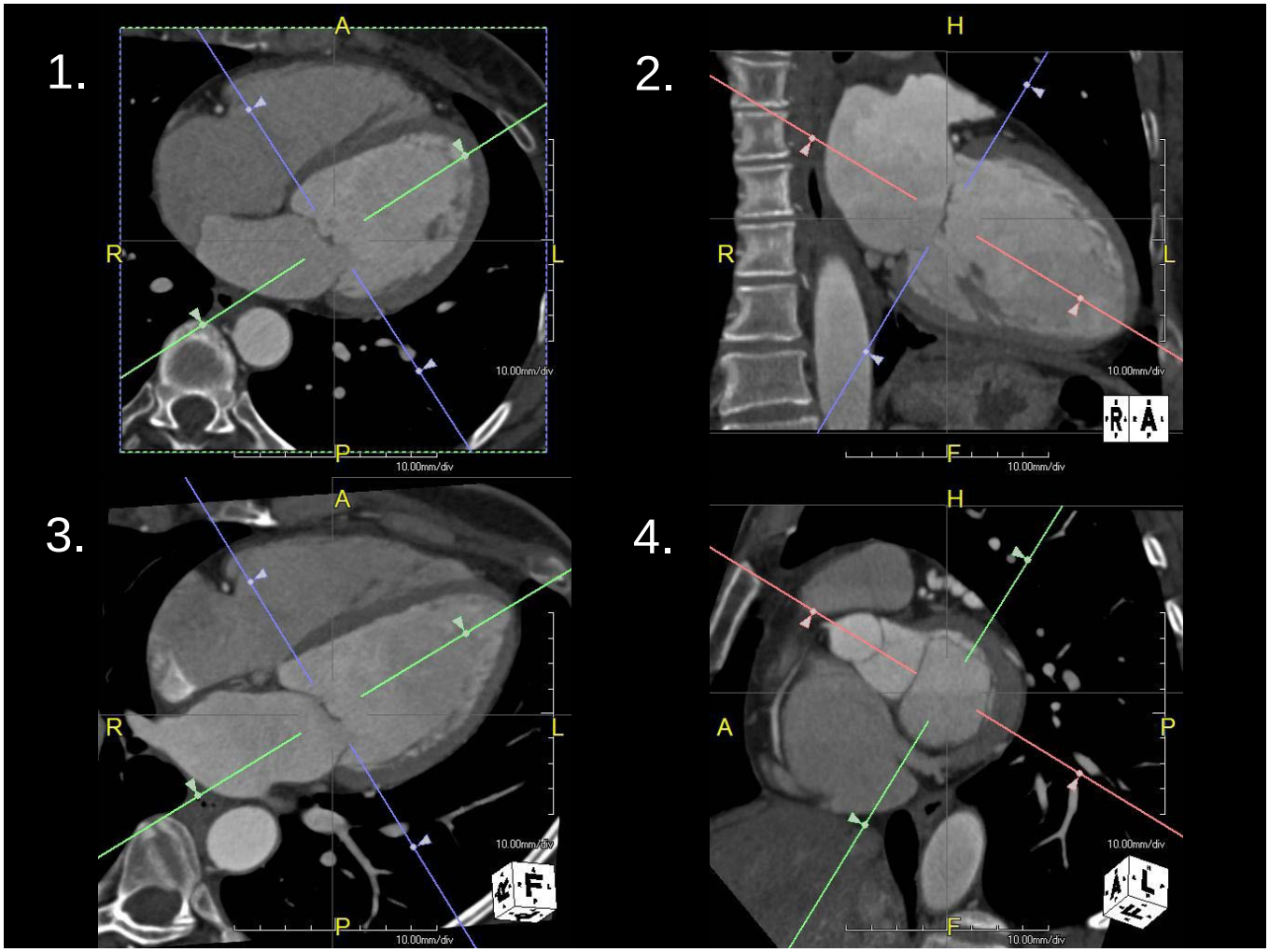

Downloaded from hyper.ahajournals.org at UNIV ZIEKENHUIS GENT POLIKLIN on October 19, 2010

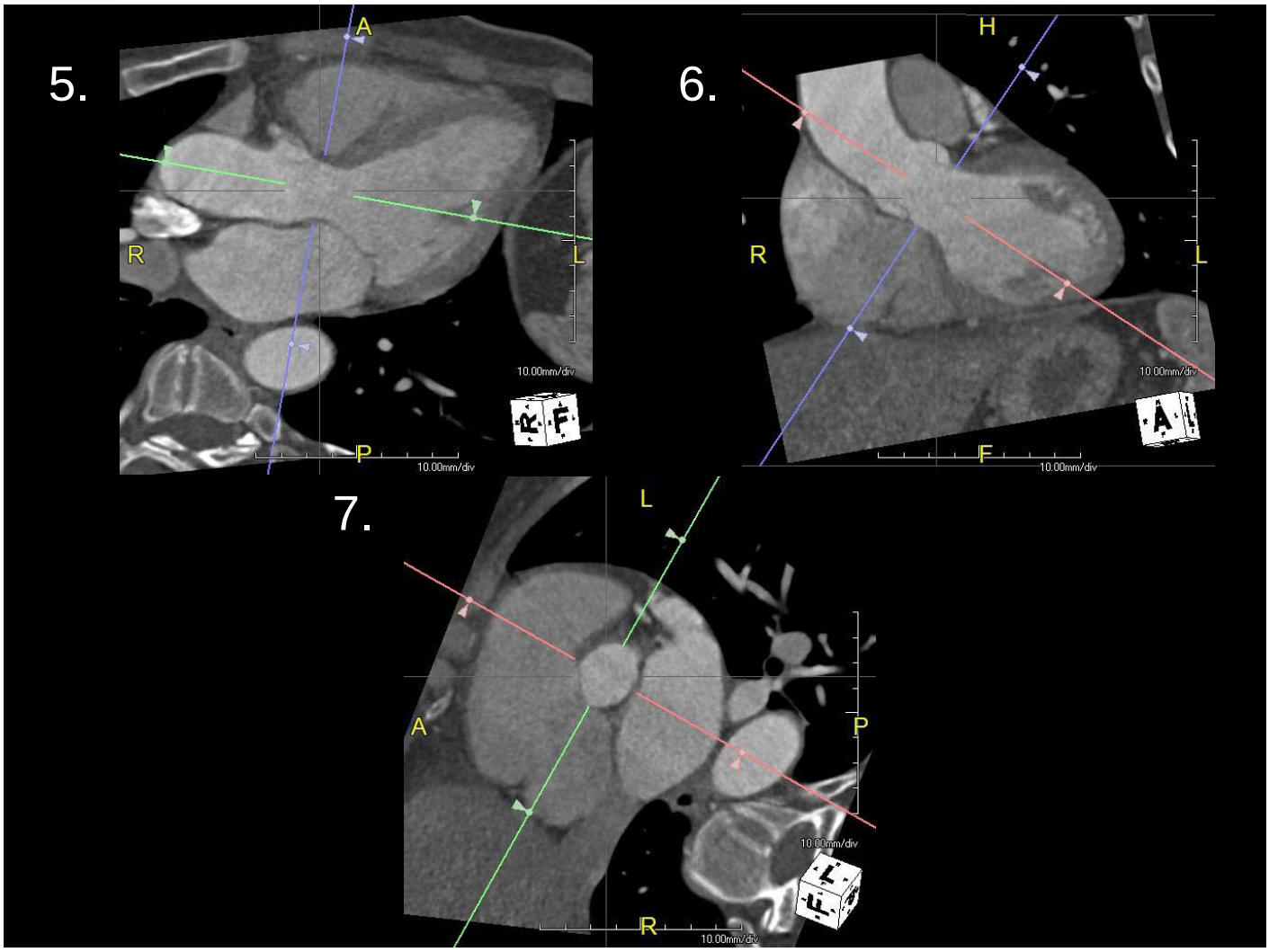

Downloaded from hyper.ahajournals.org at UNIV ZIEKENHUIS GENT POLIKLIN on October 19, 2010